Electronic Supplementary Information

Enzymatic Activity of Individual Bioelectrocatalytic Viral Nanoparticles: Dependence of Catalysis on the Viral Scaffold and its Length

Telmo O. Paiva, Angela Schneider, Laure Bataille, Arnaud Chovin, Agnès Anne, Thierry Michon, Christina Wege*, Christophe Demaille**

1- AFM-based monitoring of the decoration of TMV by the integrated system

Surface-adsorbed TMV_{Cys} virions were decorated with the Fc-PEG/PQQ-GDH integrated system by the step-by-step immunological assembly process visualized in Figure 1. The assembly was monitored by imaging the surface after each decoration step, and by measuring the particles' average height. These data are reported in Figure S1.

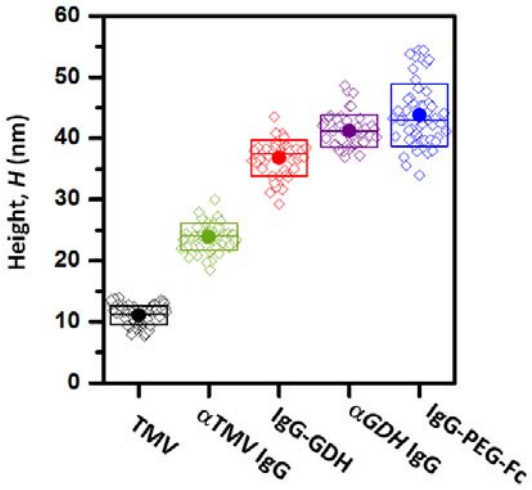

Figure S1. Apparent height of TMV particles adsorbed on SiO_2, as measured from *in situ* tapping mode AFM images, recorded at various steps of the immuno-assembly process. Data are shown for bare particles successively decorated by the anti(α)-*TMV* IgG, IgG-GDH conjugate, α-PQQ-GDH IgG and finally IgG-PEG-Fc. Note that the height was measured versus the BSA background. Open symbols are measurements of individual particles, filled symbols are average values, box height represents the standard deviation. Data were acquired using soft AFM tips home-made from flattened 25 µm gold wires. Imaging buffer: Tris-HCl pH 7.5.

One can observe that the height of the particles increased at each antibody immobilization step, indicating the effective assembly of every new antibody layer on the virions. The *H* vs. immobilization step variation is initially linear, but increases more slowly after the third antibody is immobilized on the virus capsid. This can be accounted for by the fact that, as the

number of antibody layers increases, the 3D assembly becomes increasingly flexible and is consequently less sensibly sensed by the AFM tip.

2- Extra Mt/AFM-SECM image of TMV_{cys} particles decorated by the Fc-PEG/PQQ-GDH integrated system

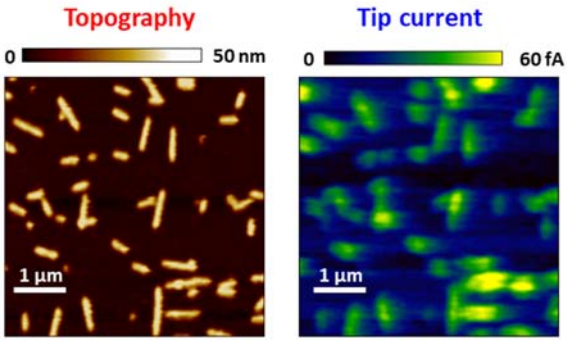

Figure S2. *In situ* tapping mode Mt/AFM-SECM images of a random array of Fc-PEG/PQQ-GDH immunodecorated TMV_{cys} particles adsorbed on a SiO_2 ultra-flat surface. The images were acquired in Tris-HCl buffer pH 7.5 containing 10 mM glucose. E_{tip} = +0.3 V/SCE. Soft home-made tips.

3- Recurring Mt/AFM-SECM images of TMV particles decorated by the Fc-PEG/PQQ-GDH integrated system before/after glucose injection.

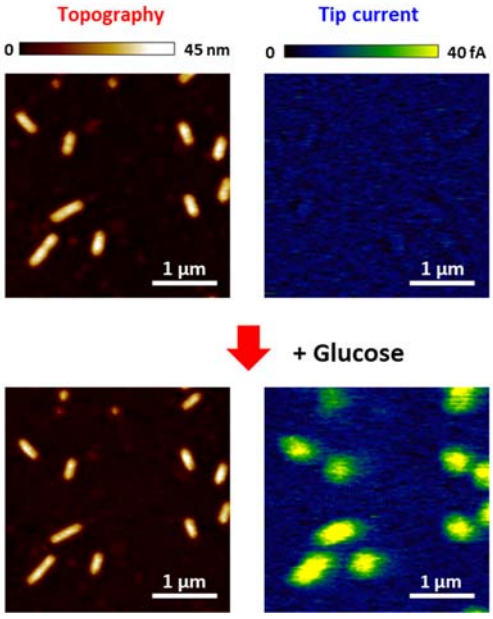

Figure S3. *In situ* tapping mode Mt/AFM-SECM images of a random array of Fc-PEG/PQQ-GDH immunodecorated TMV_{Cys} particles adsorbed on a SiO_2 ultra-flat surface. The simultaneous topography and current images were acquired for the very same particles before (top) and after (bottom) the addition of 10 mM glucose. The images were acquired in Tris-HCl buffer pH 7.5. E_{tip} = +0.3 V/SCE. Soft home-made tips.

4- Independence of the tip catalytic current from the orientation of the decorated TMV particles

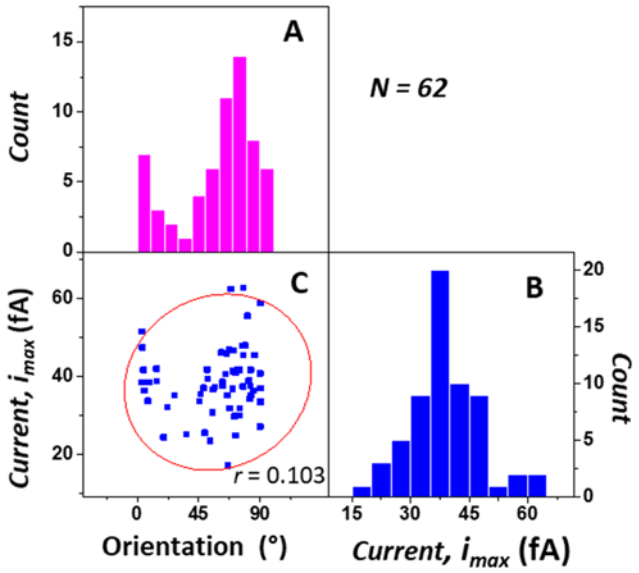

Figure S4. Searching for a dependence of the catalytic tip current, i_{max}, of individual decorated TMV particles on their orientation with respect to the tip scanning direction. Histograms of: **(A)** the particles' orientation (in degree), **(B)** catalytic tip current; **(C)**: i_{max} vs. particle orientation cross-correlation plot. The low value obtained for the Pearson's correlation coefficient, $r = 0.103$, shows that the tip current is independent from the particle orientation. The 95% confidence ellipse is shown. Soft home-made AFM-SECM probe. Imaging buffer: Tris-HCl pH 7.5 containing 10 mM glucose. E_{tip} = +0.3 V/SCE. Data acquired for $N = 62$ individual particles.

5- Measuring the linear concentration of Fc heads along the virus (γ_0) by cyclic voltammetry

A random array of TMV_{Cys} was formed onto a cysteaminated ultraflat gold surface.[1] The Fc-PEG/PQQ-GDH system was then assembled selectively onto the viral scaffolds, as described in the main text and schematized in Figure 1. A typical CV signal recorded at the gold surface bearing the decorated TMV virions is presented in Figure S5, blue trace. Also seen in this figure is the purely capacitive background signal recorded at a control surface, not exposed to the virus solution, but to BSA and sequentially to all of the antibodies, black dotted trace. One can observe that only the signal recorded at the surface bearing decorated virus particles displays a pair of peaks, centered on the standard potential of the Fc heads (~0.15 V/SCE). The surface Fc coverage (Γ_{Fc}) can be determined by integrating the anodic peak of the background-corrected CV, red trace. A value of $\Gamma_{Fc} = 1.5\ 10^{-12}$ mol/cm^2 was obtained.

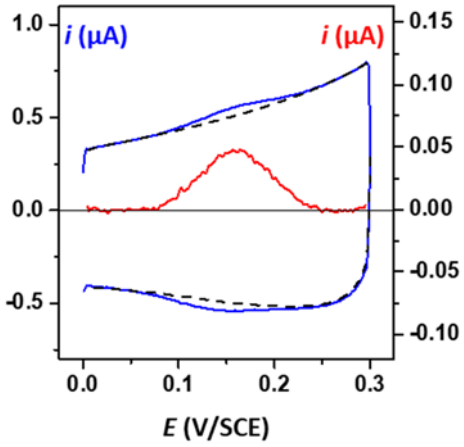

Figure S5. Blue trace: Cyclic voltammogram recorded at a gold surface bearing decorated TMV particles. Black trace: control CV recorded at a surface bearing solely the BSA blocking layer, sequentially exposed to all of the antibodies of the immunoconstruct. Red trace: background corrected CV of the TMV decorated surface, obtained by subtracting the dotted signal from the blue signal. AFM-derived TMV total length coverage 1.6 μm/μm^2. Scan rate 0.2 V/s. Tris-HCl buffer pH 7.5.

Concomitantly with the electrochemical measurements, the gold surfaces bearing the TMV-based immunoassemblies were imaged *in situ* by tapping mode AFM, in order to assess the virus coverage on the surface. However, since the TMV$_{Cys}$ particles used in this work were poly-disperse in length, the number of Fc units decorating the immunoconstructs could not be meaningfully expressed per viral particle. Instead, the Fc coverage obtained by CV was related to the *total length* of the viral particles per cm^2. In the representative case of Figure S5, AFM measurements yielded a value of 2 10^{11} nm of virus length/cm^2, which, combined to Γ_{Fc}, yielded a characteristic Fc coverage per unit of particle length of 5 ± 0.5 Fc per nm of decorated virus.

6 – Derivation of a pseudo first order rate constant, *k*, coarsely quantifying the enzyme kinetics

In the most general case, the diffusion/reaction of Fc^+ heads occurring on the decorated viral scaffold can be model by the following time-independent, 1D, 2nd Ficks law:[2]

$$D_e \frac{\partial^2 \gamma}{\partial x^2} - \frac{2k_{ox}\gamma_E \gamma}{\left(1 + K_i C_g^0\right) + \gamma\left[\frac{k_{ox}}{k_{cat}}\left(1 + \frac{K_M}{k_{cat} C_g^0}\right)\right]} = 0$$

Where x is the space coordinate measured along the virus capsid. γ *and* γ_E are the linear concentrations along the virus capsid of Fc^+ and the PQQ-GDH enzyme, respectively. γ_0 is the total Fc-head linear concentration per particle. D_e is the electron diffusion coefficient and $C^\circ g$ the glucose concentration. The individual rate constants are defined in the main text of the manuscript.

Approximating the enzyme kinetics by a pseudo first order reaction implies that the above equation becomes:

$$D_e \frac{\partial^2 \gamma}{\partial x^2} - k\gamma = 0$$

Where k is a pseudo first order rate constant, which can be coarsely approximated by:

$$k = \frac{2k_{ox}\gamma_E}{\left(1 + K_i C_g^0\right) + \gamma_0 \left[\frac{k_{ox}}{k_{cat}}\left(1 + \frac{K_M}{k_{cat} C_g^0}\right)\right]}$$

7- Dependence of the catalytic activity of individual decorated TMV_{Cys} virions on the Fc cosubstrate concentration

The most convenient way of modulating the concentration in the enzyme-active form of the Fc-cosubstrate (i.e. Fc^+) is simply to vary the electrochemical potential applied to the AFM-SECM tip. Indeed, when E_{tip} was raised from negative toward positive values, versus the standard potential of the Fc heads (+0.15 V/SCE), the Fc^+ concentration was brought from zero to its maximum value, dictated by the structure of the assembly (i.e. by the amount of IgG-PEG-Fc borne by the virion). For this, individual decorated TMV particles were imaged recursively, with the tip potential increased between each scan from -0.1 up to +0.3 V/SCE. The resulting series of topography and current images is shown in Figure S6A. The E_{tip} values set to acquire each couple of topography and current images are indicated.

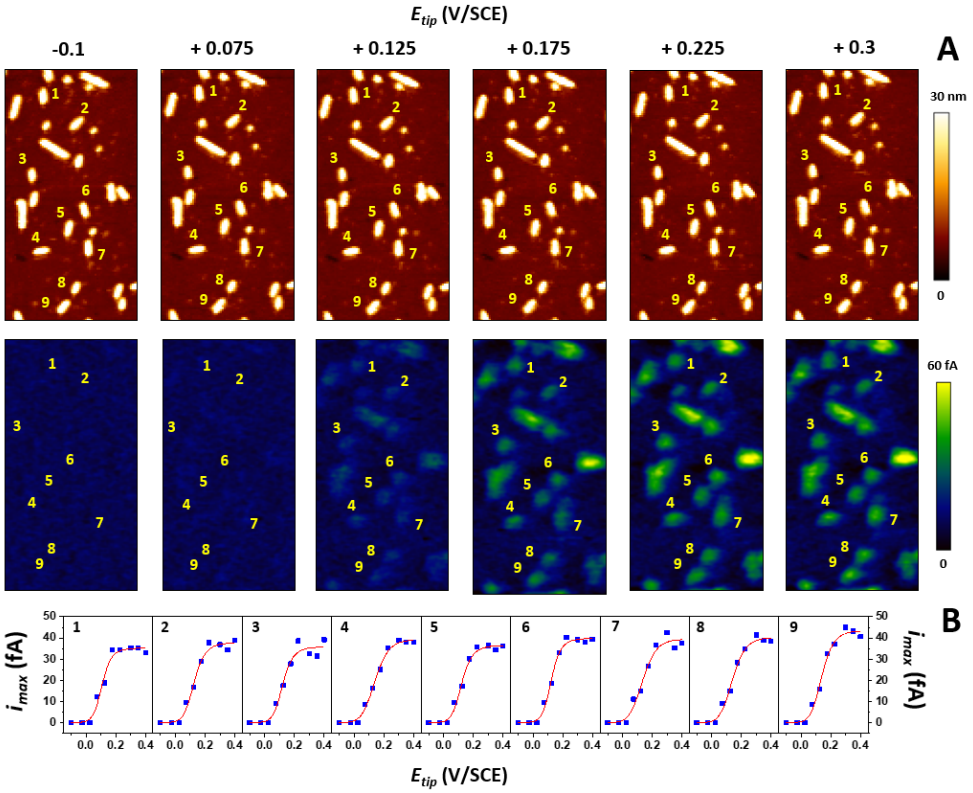

Figure S6. (A) Mt/AFM-SECM 3 µm x 6 µm images of individual Fc-PEG/PQQ-GDH decorated TMV particles recorded at various tip potential values, E_{tip}, as indicated on the top of the images. The very same virions were imaged recursively after incrementing the tip potential value. Nine particles belonging to the monomeric TMV population were selected and labeled from 1 to 9 as shown. **(B)** Tip CV plots showing the variation of the catalytic tip current, i_{max}, as a function of E_{tip}, for each of the nine indexed particles. The red lines are guides to the eyes. The images were acquired in Tris-HCl buffer pH 7.5 containing 10 mM glucose, using AFM-SECM soft tips. For clarity, only 6 out of a total of 10 topography-current image pairs, corresponding to differing E_{tip} values, are presented.

In the topographic images, numerous individual virions are resolved well and neither their position, appearance, nor height were altered by the change in E_{tip} and repeated imaging. Examining the current images, it can be observed that whereas the image acquired with E_{tip} = -0.1 V/SCE displays only noise, spots associated with the particles visible in topography progressively appear, and become more visible as the tip potential is raised. More precisely, the spots become discernible from E_{tip} > 0.075 V, their intensity increases as E_{tip} is raised up to 0.225 V/SCE, and remains unchanged when E_{tip} is further raised to 0.3 V/SCE.

From these images, nine virions were identified as pertaining to the population of monomeric TMV and labeled from 1 to 9. The intensity of the catalytic tip current associated with each of these particles is plotted as a function of E_{tip} in the "tip voltammograms" shown in Figure S6B. These S-shaped CVs seemingly bear a large degree of similarity. Most notably,

for each of them, one can estimate a potential at mid height of 0.13 ± 0.01 V/SCE, corresponding nicely to the standard potential of the PEG-attached Fc moieties. This result confirms that the Fc heads of the integrated system are the only mediators of the enzymatic catalysis probed by the tip. In order to further analyze the degree of similarity of the CVs recorded for distinct particles, cross-correlation plots were constructed, where the current values of the different particles were plotted as function of each other, see Figure S7.

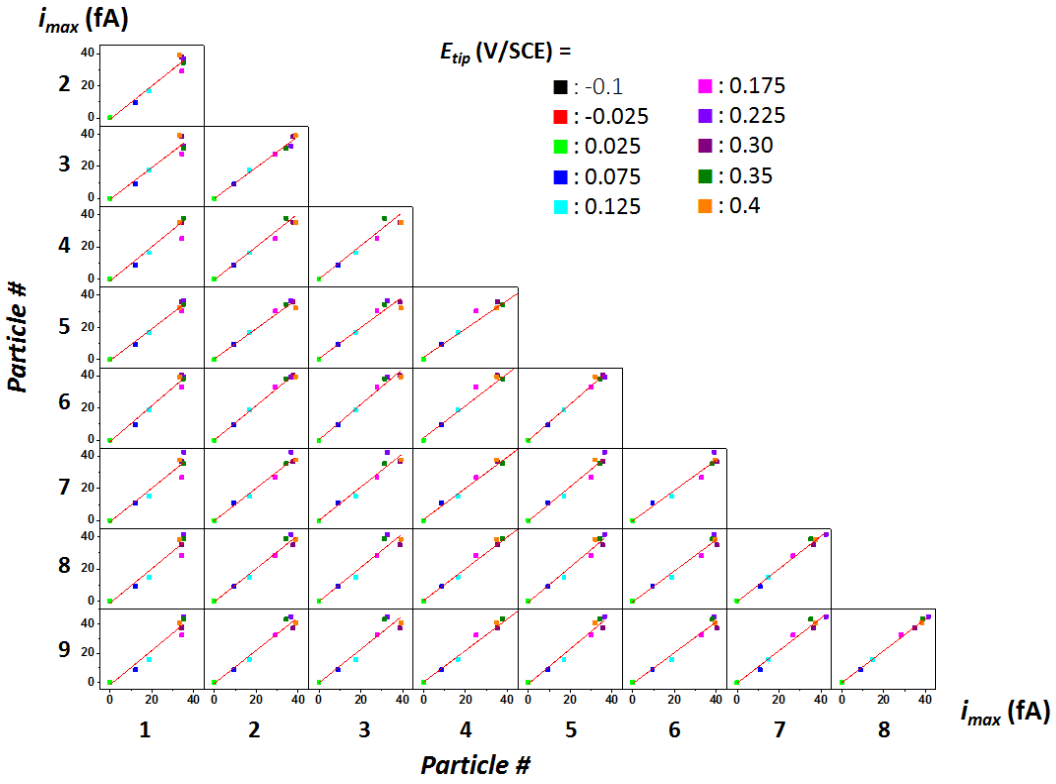

Figure S7. Cross-correlation plots where the catalytic tip current, i_{max}, of the particles labeled 1-9 in Figure S6, is plotted as a function of each other, for every E_{tip} values explored. Red traces are least square regression lines passing through the origin. Imaging buffer Tris pH 7.5, containing 10 mM glucose. E_{tip} = + 0.3 V/SCE.

Remarkably, the data points all align on straight lines passing through the origin, evidencing that all of the CVs are simply proportional to each other. This result evidences that the catalytic behavior of all the virions interrogated have exactly the same dependency on the Fc^+ concentration. It can thus be concluded that the PQQ-GDH molecules borne by these different particles display identical kinetics regarding their oxidation by Fc^+. This observation legitimates the notion of deriving an average CV, characteristic of the Fc^+ dependence of the catalytic response of the decorated TMV virions, simply by averaging the signals presented in Figure S6B. Such a representative CV is shown in Figure S8. It contains information regarding the kinetics of PQQ-GDH acting within the integrated system that could, in principle, be extracted by a proper quantitative analysis.

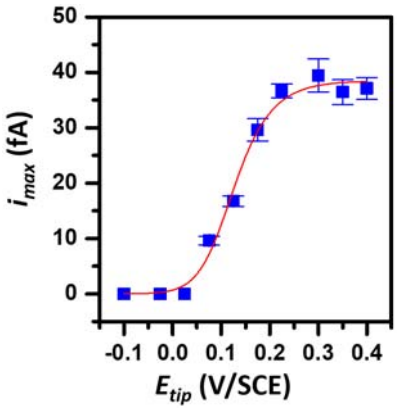

Figure S8. Kinetic curves characterizing the catalytic activity of the TMV-scaffolded Fc-PEG/PQQ-GDH integrated system. i_{max} values corresponding to 8 distinct TMV particles were averaged yielding the average CV shown. This CV captures the dependence of the catalytic tip current on the tip potential, E_{tip}, which sets the Fc^+ concentration.

Yet this would require deriving the exact value of the Fc^+ concentration as experienced by the enzyme from the value of the tip potential. The problem is that this concentration *a priori* also depends on the rate of Fc^+ production at the tip, which, apart from the plateau region of the CV where it is infinitely fast, depends on the tip potential in an unknown way. Hypothesis regarding this rate dependence would have to be made in order to analyze the average CV, and we did not resort to make them.

8- Comparison of the tip current vs. glucose concentration kinetic plots obtained for the *fd*- and TMV-scaffolded integrated systems, respectively.

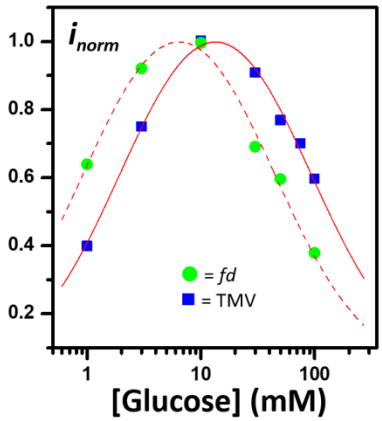

Figure S9 Normalized tip current vs. glucose concentration kinetic plots obtained for the *fd*-, (●), and the TMV-(■)scaffolded integrated systems. The curves in red are best fits of equation (4) to the series of data.

9- Assaying the linear GDHcoverage of TMV, γ_E

The amount of GDH molecules decorating TMV_{Cys} was quantified by assaying the PQQ cofactor stripped from SiO_2 surfaces bearing the decorated TMV nanoarrays, as described previously.[1]

After complete assembly of the Fc-PEG/PQQ-GDH system on the viral particles, 0.1 M glycine buffer pH 2.5 was left in contact with the surface for 90 min, in order to strip off the antibodies from the viral nanoarrays into a small volume (20µL). This drop was collected and the surface was subsequently rinsed twice with 20 µL of Tris-HCl buffer pH 7.5. Once collected, the three drops were pooled and brought to 100 µL by adding the required volume of 0.1 M Tris-HCl buffer pH 7.5. The 100 µL sample was then heated in a circulation water bath at 50°C for 60 min, denaturing the GDH and promoting the spontaneous release of its PQQ cofactor molecules.[16]

Apo-GDH was added in excess (25 nM) compared to the amount of PQQ in the sample. The apo-GDH spontaneously reconstituted into its active holo-GDH form by incorporating the PQQ in the sample, and the enzymatic activity was measured spectrophotometrically in the presence of glucose and two soluble redox cofactors (phenazine methosulphate (PMS) and 2,6-dichlorophenolindophenol (DCPIP)).[3] The absorbance of DCPIP, which acts as a terminal electron acceptor of the redox chain, was measured at 605 nm immediately after glucose addition. The initial discoloration rate, corresponding to the enzyme-catalyzed consumption of DCPIP, was converted into an actual PQQ concentration in the sample, based on calibration assays of test PQQ samples.

The amount of GDH molecules per μm^2 of surface was calculated, taking into account that two PQQ molecules are released per GDH, and considering the geometric area of the SiO_2 surface. Due to the polydisperse length of the TMV_{Cys}, the enzyme coverage on the virions had to be expressed by the number of GDH molecules per unit length of virus. To this end, the length of virus per unit surface area was assessed by *in situ* AFM. The linear enzyme coverage of TMV_{Cys} could then be derived, yielding a typical value of $\gamma_E = 0.1 \pm 0.02$ GDH molecules per nm of decorated virus.

10- Extra Mt/AFM-SECM zoomed-in image of a decorated DTLP

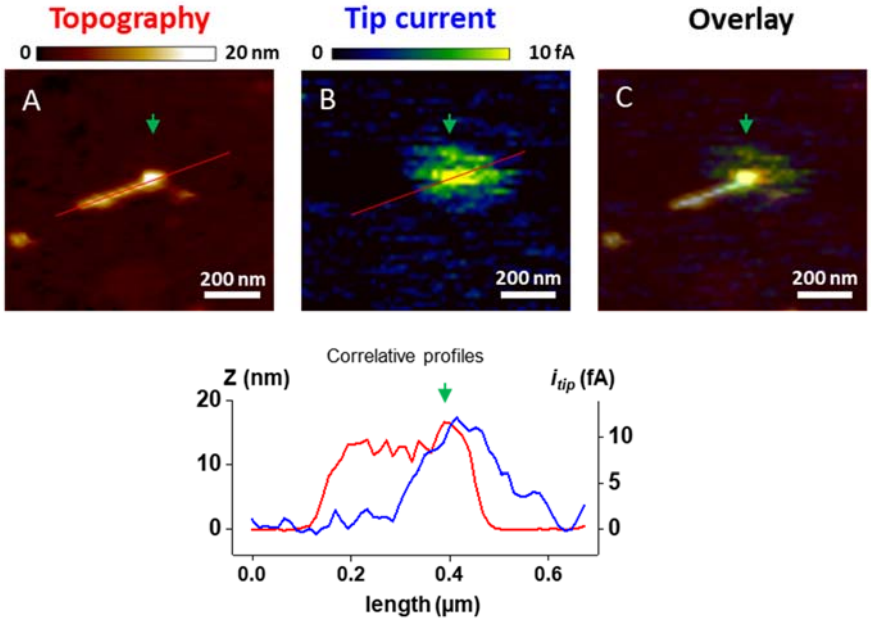

Figure S10. Mt/AFM-images of an individual $CP_{Cys}/CP_{Cys\text{-}bio}$ DTLP terminally decorated by the Fc-PEG/PQQ-GDH system. **(A)** Topography image. **(B)** Current image. **(C)** Overlaid topography and current images. Topography and current profiles taken along the long axis of the virion, as shown in A and B, are reproduced below the images. The green arrow marks the approximate position of the 40 nm long $CP_{Cys\text{-}bio}$ extremity of the viral particle. Soft AFM-SECM tip. Imaging buffer: Tris-HCl pH 7.5 containing 10 mM glucose. E_{tip} = +0.3 V/SCE.

11- Zoomed-in Mt/AFM-SECM images of decorated TMV particles.

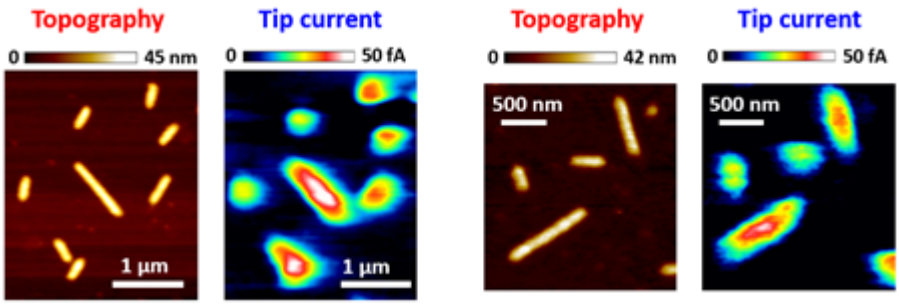

Figure S11. Zoomed-in Mt/AFM-SECM images of individual TMV particles decorated by the Fc-PEG/PQQ-GDH system. Images acquired using soft AFM-SECM gold tips. Imaging buffer: Tris-HCl pH 7.5 containing 10 mM glucose. E_{tip} = +0.3 V/SCE.

12- Characteristics of the flexible gold AFM/ AFM-SECM probes

The AFM-SECM probes were prepared from 99.99% pure gold wires, of either 60 µm (old probes) or 25 µm (new probes) in diameter, following an already reported protocol.[4] This process starts by flattening the wire between stainless steel jaws, to forms the flat and flexible cantilever arm of the probe, as shown in Figure S12 for a 60 µm (A) and a 25 µm wire (B).

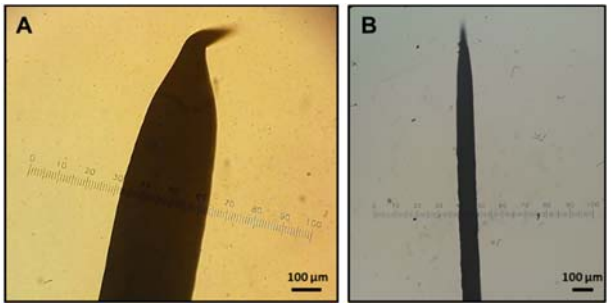

Figure S12. Optical microscopy images of a flattened **(A)** 60 µm and **(B)** 25 µm diameter gold wire forming the cantilever arm of the probe. Magnification 10x.

For a 60 µm wire the arm width is typically of 300 µm, and of only 100 µm for the new probes. The bent portion of the tip, the "nose", is then etched to a sharp cone as shown in Figure S13. Note that the "nose" length is ~300 µm long, which avoids shielding of the surface by the cantilever arm.

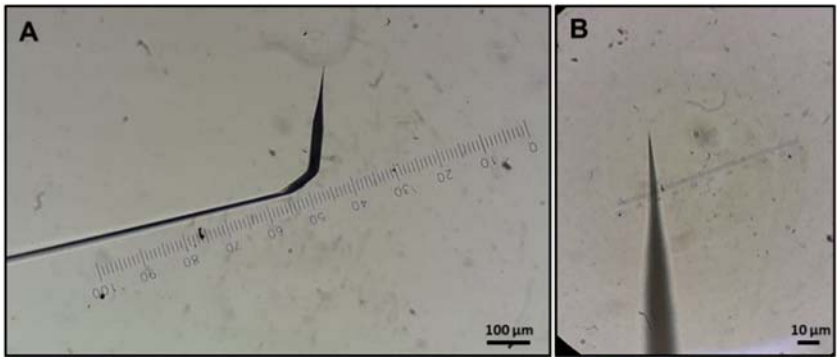

Figure S13. Optical microscopy images of a gold probe (25 µm wire) after electrochemical etching, showing **(A)** the flexible arm and the nose. Magnification 10x. **(B)** Detail showing the sharpened nose extremity (tip). Magnification 100x.

If to be used in AFM-SECM, the probe is insulated by deposition of electrophoretic paint, as described earlier.[4]

The probe is then glued onto a plastic chip, keeping about 1-1.5 mm of the cantilever overhanging. Spring constants of individual probes can then be determined by recording thermal excitation spectra on the AFM setup (Figure S14).

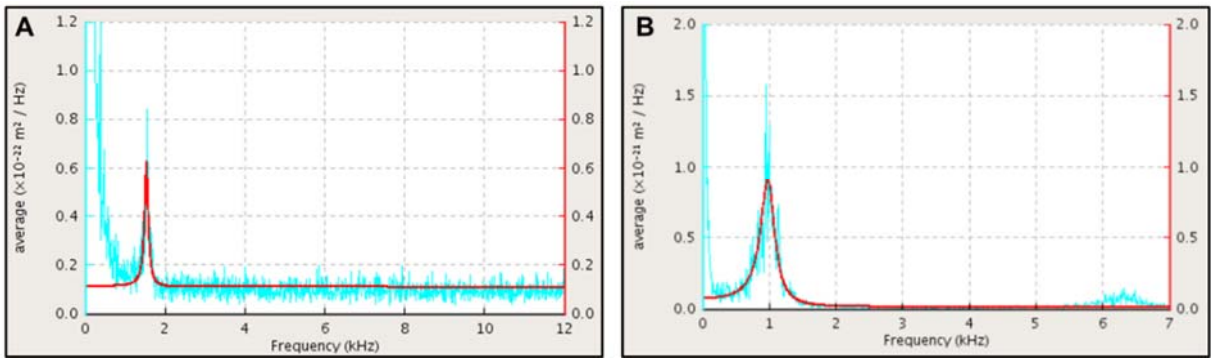

Figure S14. Thermal noise spectra showing the measured cantilever resonance peak (blue) and the Lorentz fit (red) of an AFM-SECM cantilever made from a **(A)** 60 µm and **(B)** 25 µm diameter gold wire. Spectra were acquired in liquid (aqueous). **(A)** f = 1.5 kHz; **(B)** f = 1.0 kHz.

Spring constants of 4 N/m and 0.1 N/m were found for the probes corresponding to the spectra presented in Figure S14A (old probe) and S14B (new soft probe), respectively.

Occasionally, SEM images of the probe extremity can be taken (Figure S15). They typically display tip radius of curvature in the ~50 nm range.

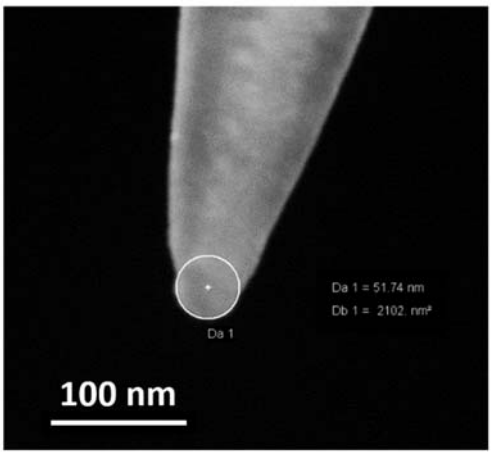

Figure S15. Scanning electron microscopy image of the very end of a home-made AFM-SECM gold tip.

13- Effect of tip convolution on the Mt/AFM-SECM images

The tip-particle convolution effect is responsible for the difference between the dimensions of objects as they appear in AFM images and as they really are. This artifact is commonly observed in all the AFM-related techniques. Thus, the dimensions of the TMV particles imaged throughout this work are dependent on the radius of the AFM-SECM probe used. Although we attempted to minimize these effects, by using a very small set of AFM-SECM tips, all

displaying the same geometrical features, it is worth discussing how both the AFM-SECM topography and current images were affected by tip convolution effects.

The apparent width of the particles, measured by taking a profile across the particles, was much more affected by convolution than their length. This was true for both the topography and current images, as is illustrated in Figure S16A and S16B, respectively.

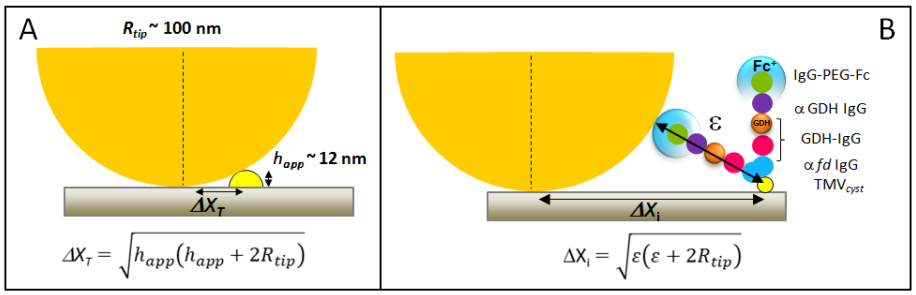

Figure S1.6 Schematics showing how the tip-object convolution artifact enlarges the apparent width of the decorated particles as seen in topography **(A)** or in current **(B)** images. The schemes are drawn to scale, with a tip ~ 100 nm radius, and considering IgGs and GDH as spheres, 15 nm in diameter, as depicted in (B). It is assumed the Fc^+ heads can explore a space region (colored in a light blue gradient) extending ~ 10 nm around the PEGylated IgG. The *fd* particles are predicted to display apparent widths of $2\Delta X_T$ and $2X_i$, in the topography and current images, respectively.

- In topography, the tip-particle convolution yields an apparent particle width $2\Delta X_T$, related to the apparent particle height, h_{app}, and tip radius, R_{tip}, by the equation reproduced in Figure S16A. For bare TMV particles, taking h_{app} = 11 nm (as derived from the actual topography images given in the main text), and taking R_{tip} ~50-100 nm, yields an apparent particle width of ~70-100 nm, respectively, in reasonable agreement with the particle width values measured from the topography images reproduced in Figure 1B (80 nm). Rationalizing the width of the decorated particles on the basis of the above equations is made more ambiguous because the IgG coating contributes to the particles width to some unknown extent, due to its intrinsic flexibility.

- In current, the tip-particle convolution results in an apparent particle width $2\Delta X_i$, related to the tip radius and the effective height of the immune-assembly, ε, as shown in Figure S16B. The ε value can be coarsely estimated by considering: (i) IgGs and GDH as spheres, 15 nm in diameter, and (ii) that the Fc^+ heads can efficiently explore a space region extending ~10 nm around the PEGylated IgG.[14] This yields ε = 100 nm, and taking R_{tip} ~50-100 nm, an apparent "electrochemical" width of the particle of ~ 200-350 nm. This range can be compared to the particle width measured on zoomed-in current images of decorated TMV since (such as shown

in Figure S11). From these images a typical decorated particle width of ~400 nm is found, which slightly exceeds the expected width range.

➔ Understandably, when the tip is scanned toward the particles and approaches from their edges, i.e. the region where tip convolution effects are sensed, the tip-particle contact area increases progressively and so does the current. Yet, as explained in the text, the catalytic tip current was measured along current profiles taken in the *center line* of the particles, in a region where the tip extremity sits *entirely* above the decorated parties, since the tip radius is less than the actual full width of the decorate particle (2ε = 200nm). As a result, tip convolution effects do not affect i_{max} measurements.

References

[1] K. Torbensen, A. N. Patel, A. Anne, A. Chovin, C. Demaille, L. Bataille, T. Michon, E. Grelet, *ACS Catal.* **2019**, *9*, 5783.

[2] T. O. Paiva, K. Torbensen, A. N. Patel, A. Anne, A. Chovin, C. Demaille, L. Bataille, T. Michon, *ACS Catal.* **2020**, *10*, 7843.

[3] F. Durand, C. Stines-Chaumeil, V. Flexer, I. André, N. Mano, *Biochem. Biophys. Res. Commun.* **2010**, *402*, 750.

[4] J. Abbou, C. Demaille, M. Druet, J. Moiroux, *Anal. Chem.* **2002**, *74*, 6355.